AIAA JOURNAL
Vol. 49, No. 4, April 2011

Tuned Passive Control of Acoustic Damping of Perforated Liners

Dan Zhao*
University of Cambridge, Cambridge, England CB2 1PZ, United Kingdom
Aimee S. Morgans†
Imperial College London, London, England SW7 2AZ, United Kingdom
and
Ann P. Dowling‡
University of Cambridge, Cambridge, England CB2 1PZ, United Kingdom

DOI: 10.2514/1.J050613

To suppress combustion instabilities, perforated liners can be fitted along the bounding walls of a combustor to provide acoustic damping. These liners are typically subjected to a low-Mach-number bias flow (a cooling flow through perforated holes), and they tend to be effective only over narrow frequency ranges. To investigate the damping effect of perforated liners on plane acoustic waves and to increase their effective frequency range, experiments and numerical simulations are carried out. An acoustically driven pipe system containing a lined section was designed and experimentally tested. The length of the pipe system, along with the bias flow rate, could be varied. The experimental results showed that the liner damping depended on both the pipe length and the bias flow rate, in agreement with predictions from the numerical model presented by (Eldredge, J. D., and Dowling, A. P., "The Absorption of Axial Acoustic Waves by a Perforated Liner with Bias Flow," *Journal of Fluid Mechanics*, Vol. 485, No. , 2003, pp. 307–335.). To maintain the acoustic damping of the liner in the presence of large frequency changes (corresponding to instability frequency changes in a combustor), real-time tuning of perforated liners was experimentally investigated. Both a pipe length parameter and the bias flow rate were sequentially tuned using a multiple-parameter tuning scheme. The scheme required two algorithms to be developed: one for characterizing the liner's acoustic damping in real time and another for sequentially determining the two optimum actuation signals for the damper tuning. The former involved developing a real-time version of the two-microphone technique for resolving the two plane acoustic wave strengths, which is widely applicable. On implementing these algorithms in the pipe system, optimal damping of the liner was achieved and maintained over a broad frequency range.

I. Introduction

MORE stringent requirements on emissions mean that combustors in ground-based gas turbines and aeroengines need to operate under lean premixed conditions in order to achieve low NOx. However, under lean premixed conditions, combustors are more susceptible to combustion instabilities. Combustion instabilities [1] are generated by an interaction between acoustic waves and unsteady combustion. Unsteady heat release is an efficient acoustic source and generates acoustic waves. These pressure waves propagate within the combustor and partially reflect from boundaries to arrive back at the combustion zone, where they cause more unsteady heat release. Under certain conditions, this feedback can result in large and damaging self-excited oscillations.

To suppress combustion instabilities, the coupling between unsteady heat release and the pressure perturbation must somehow be interrupted. Perforated liners along the bounding walls of a combustor can be used as acoustic dampers; they dissipate acoustic waves, preventing further perturbations in heat release. The liners are typically made of metal, are arranged in layers, and have tiny perforated holes in them [2–5]. In practice, a cooling air flow through the perforated holes (known as a bias flow) is needed to prevent the liners from being damaged by high temperatures (see Fig. 1). Remarkably, the bias flow is found to increase liner damping performance [6,7]. Their main damping mechanism involves vortex shedding generated over the rims of the perforated holes [8]. One current drawback of such liners is that they tend to be effective over a limited frequency range and cannot respond to changes in operating conditions.

The perforated holes are too small to simulate accurately in most computational codes, and so analysis of perforated liners is currently restricted to modeling, measurement, and specialized direct numerical simulations (DNSs). Tam et al. [9] carried out time-domain DNS of a single liner and showed that vortex shedding is the dominant mechanism of absorption for incident waves of high amplitude. Reichert and Biringen [7] proposed a time-domain approach that introduced a source term to the momentum equations, and they assessed the effect of a bias flow numerically. They found that, with an optimum bias flow rate, the liners damping efficiency was significantly improved over that with no bias flow. This finding, shared by Follet et al. [6], has supported the idea of tuning the bias flow rate to improve the liner damping performance.

The majority of modeling work has been carried out in the frequency domain. Howe [10] modeled the acoustic energy dissipated by the periodic shedding of vorticity for a single orifice in a high-Reynolds-number flow using a Rayleigh conductivity. Following Howe's research, Hughes and Dowling [11] studied the acoustic damping of screens with a regular array of slits and circular perforations with mean bias flow, showing that all impinging sound could be absorbed at a particular frequency in theory. Jing and Sun [4] experimentally investigated the effect of the screen thickness and the bias flow rate, showing that an appropriate bias flow rate can significantly increase damping and that the screen thickness is crucial.

Presented as Paper 2009-3406 at the 15th AIAA/CEAS Aeroacoustics Conference, Miami, FL, 11–13 May 2009; received 19 April 2010; revision received 28 September 2010; accepted for publication 6 December 2010.

*Currently, Aerospace Engineering Division, College of Engineering, Singapore 639798; Zhaodan@ntu.edu.sg. Member AIAA.
†Lecturer, Department of Aeronautics. Member AIAA.
‡Professor, Department of Engineering. Member AIAA.

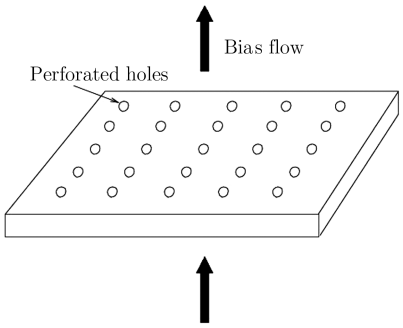

Fig. 1 Schematic of typical perforated liner/plate.

Much of the preceding work concluded that the choice of bias flow rate was crucial to obtain the best possible damping performance from a given liner. The recent modeling and experimental work of Eldredge and Dowling [2] developed this idea further. They used a one-dimensional duct model with a homogeneous liner compliance to numerically simulate a loudspeaker-driven cold-flow pipe system. Both the bias flow rate and the loudspeaker forcing frequency were varied. They found that the liner damping was strongly dependent on the bias flow rate at some frequencies (e.g., 273, 473, and 647 Hz), but at others (e.g., 374 Hz), the bias flow rate had little effect. Their analysis also showed that the liner damping was dependent on not only the bias flow rate but also on the position of the liner along the pipe.

In this work, both experiments and numerical simulations are carried out: first, to investigate the damping effect of perforated liners, and second, to increase their effective frequency range using tuned passive control [12,13]. Our experimental setup is based on that of Eldredge and Dowling [2], but in our case, both the pipe length and the bias flow rate are made variable. In Sec. II, the experimental setup is described, and the dependence of the liner damping (defined in different ways) on the pipe length and the bias flow rate is discussed. In Sec. III, the numerical model of Eldredge and Dowling [2] is used to simulate the experiments. This uses a homogeneous liner compliance embodying the liner damping mechanism to couple the linearized flow conservation equations across the liner. The numerical and experimental results are compared, and design guidance insights for optimizing the liner damping performance are extracted. Finally, in Sec. IV, in order to broaden their effective frequency range, the tuning of perforated liners was experimentally investigated. Both the pipe length parameter and the bias flow rate were varied simultaneously using a multiple-parameter tuning scheme. This involves developing algorithms for characterizing the liner damping in real time and for determining the optimum bias flow rate and the pipe length. The former algorithm involved developing a real-time version of the two-microphone technique for resolving the two plane acoustic wave strengths, which is widely applicable. On implementing these algorithms, it was found that the optimum damping was achieved and maintained over a broad frequency range.

II. Description of Experiment

A. Experimental Setup

To investigate the acoustic damping of a perforated liner, a cold-flow axial pipe system containing a small length of double-layer liner was experimentally set up, as shown schematically in Fig. 2. The pipe system had no imposed mean flow passing through it. Both the bias flow rate through the liner and the pipe length to one side of the lined section were made variable.

The double-layer liner (with thickness of 3 mm) was encased in a large cavity, as shown in Fig. 3b. A controllable supply of air was fed into the cavity by a centrifugal pump to produce bias flow through the liner (measured by a pitot probe in the cavity inlet). The measured flow rate was then used to calculate the corresponding bias flow rate through the perforated holes. In this way, the bias flow rate was calibrated from 0 to 12 m/s. The centrifugal pump was controlled by an analog output channel through a four-channel DMX dimmer pack.

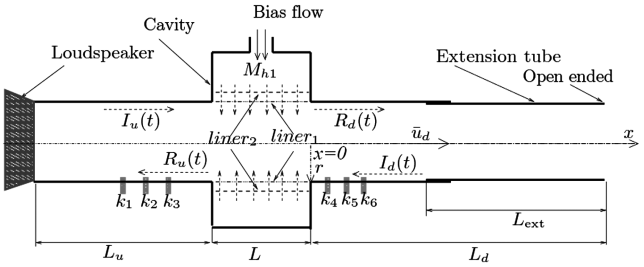

Fig. 2 Schematic of experimental setup.

The centerlines of the perforated holes in the inner liner were tilted at an angle by approximately 45°, so that the flow passing through them would travel in the absence of a mean pipe flow.

A loudspeaker with an amplifier was attached to one end of the pipe to generate acoustic waves in the pipe with a magnitude between 90 and 140 dB and a frequency between 300 and 700 Hz. This frequency range was well below the cut-on frequency of the first radial mode of approximately 3300 Hz. The pipe to the other side of the lined section was open and consisted of a fixed-length piece and an extension piece, as shown in Fig. 3a. The extension piece could be moved horizontally along the tube axis by a Maxon direct current (DC) motor (controlled by an EPOS24/5 controller), as shown in Fig. 3c. This made the downstream pipe length L_d variable from 1.32 to 1.78 m.

Three pressure sensors (Kulite transducers) were placed on the tube sections to either side of the liner. The Kulite transducers (hereafter referred to as Kulites) were calibrated by a calibration box and piston phone (124 dB at 250 Hz) before being used, as shown in Fig. 3c.

The geometry of the liners and the experimental setup, and the positions of pressure transducers (Kulites), are summarized in Table 1. Here, x_1 to x_6 denote the axial positions of the Kulite sensors, and L_u denotes the length of the pipe upstream of the liner (i.e., containing the loudspeaker forcing). Note that there is no mean flow through the pipe, but the end containing the loudspeaker will be referred to as the upstream end. L_d denotes the pipe length to the other side of the liner (which includes both the fixed and extension tube lengths), L_{ext} and D_{ext} denote the extension length and its internal diameter, respectively, L is the liner length, D_1, D_2, δ_1, and δ_2

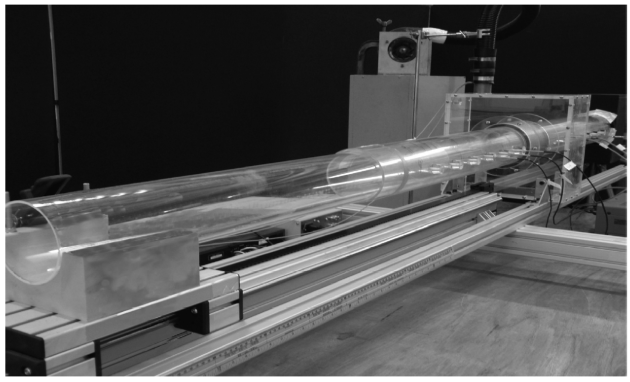

a) Experimental rig

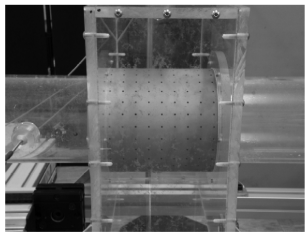

b) Double-liner section

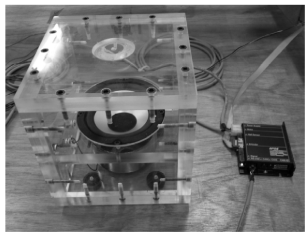

c) Calibration box and controller

Fig. 3 Experimental rig setup, double-liner lined section, Kulite calibration box, and Maxon DC motor controller.

Table 1 Geometry of the experimental pipe system

Parameter	Value	Parameter	Value
x_1	−0.578 m	d_1	0.75 mm
x_2	−0.478 m	D_2	0.152 m
x_3	−0.378 m	d_2	3.0 mm
x_4	0.1 m	T	293.0 K
x_5	0.2 m	$\bar{M}_{h1}$	0.0–0.036
x_6	0.3 m	D_{ext}	0.125 m
x_u	−0.958 m	L	0.178 m
S_p	0.0127 m^2	L_d	1.32–1.78 m
δ_1	0.04	L_{ext}	1.0 m
δ_2	0.02	L_u	0.78 m
D_1	0.127 m		

are the diameters and open-area ratios of the inner and outer liners, respectively, $\bar{M}_{h1}$ is the bias flow Mach number through the inner liner holes, d_1 and d_2 are the diameters of the perforated holes of the inner and outer liners, respectively, S_p is the pipe cross-sectional area, and T is the measured temperature.

A LabVIEW program was developed to vary the downstream length and the bias flow rate and to acquire pressure measurements. The pressure perturbations measured by the Kulites are used to determine the amplitudes of the incident and reflected waves upstream and downstream of the liner [i.e., $I(t)$ and $R(t)$], as shown in Fig. 2, using the two-microphone technique [14–16].

B. Preliminary Investigations

Initial investigations were carried out to study the effect of varying the downstream pipe length and the bias flow rate on the acoustic damping of the perforated liner. The acoustic damping can be characterized by either considering the pressure amplitude at a given location or by considering the acoustic wave energy being absorbed (i.e., power absorption). Power absorption Δ is defined in terms of the incident and reflected waves on either side of the lined section, as shown in Eq. (1). Theoretically, the achievable maximum power absorption is approximately 83%, as shown by [2]. Here, $\hat{I}(\omega)$ and $\hat{R}(\omega)$ denote the Fourier transforms of the incident and reflected wave amplitudes $I(t)$ and $R(t)$, respectively, in Fig. 2. One can envisage many situations where absorbing the most acoustic power would be the aim:

$$\Delta = 1.0 - \frac{|\hat{R}_d(\omega)|^2 + |\hat{R}_u(\omega)|^2}{|\hat{I}_u(\omega)|^2 + |\hat{I}_d(\omega)|^2} \tag{1}$$

There are many other situations, such as in a combustor, where (instead) it may be desirable to minimize the pressure amplitude at a given location, such as the flame location. For this reason, the

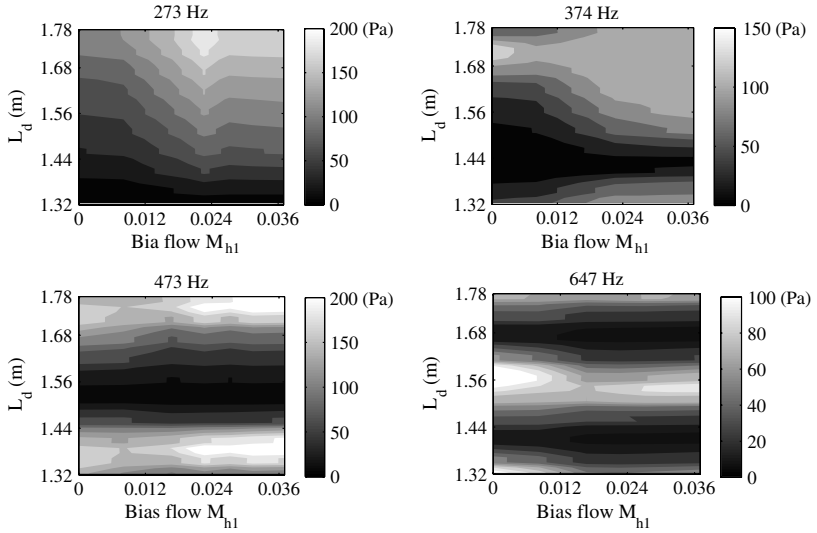

Fig. 4 Variations of pressure amplitude with downstream pipe length L_d and bias flow Mach number M_{h1}, as measured experimentally.

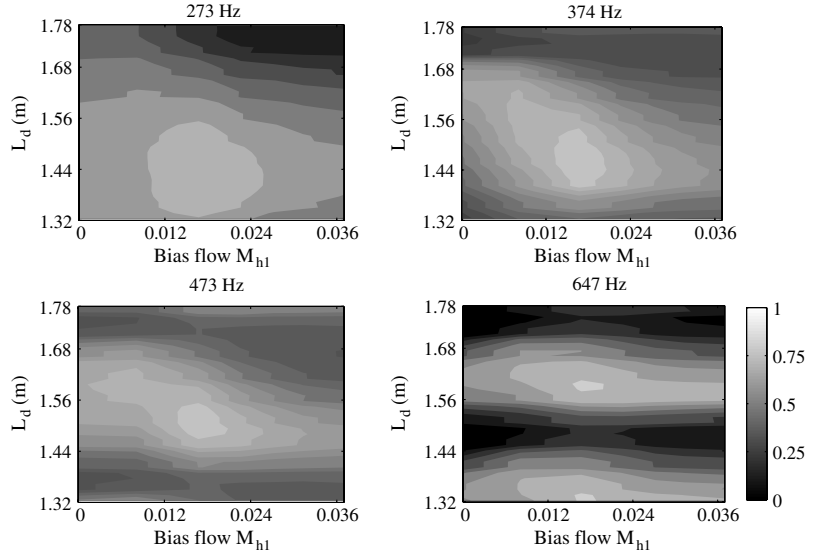

Fig. 5 Variation of power absorption with downstream pipe length L_d and bias flow Mach number M_{h1}, as measured experimentally.

preliminary investigations considered the effect of downstream length and bias flow rate on both power absorption and pressure amplitude at a given location.

Considering first the variation of pressure amplitude at a given location, chosen to be k_4, the effect of varying the downstream pipe length and bias flow rate was experimentally measured and shown in Fig. 4 at four different frequencies. It can be seen that the pressure amplitude can be reduced to approximately 0 Pa at each frequency, as long as the downstream pipe length is properly chosen. This reveals that the pressure amplitude depends on downstream pipe length much more strongly than on bias flow rate: the latter having little effect on the pressure amplitude minima, for which the location is independent on the presence of the lined section (or bias flow). This is due to the constructive interference between the incident and reflected waves [8].

Considering now the variation of power absorption with the downstream length and the bias flow rate, this was experimentally measured and shown in Fig. 5. It can be seen that the power absorption can be increased to approximately 80% at each frequency, when both the downstream pipe length and the bias flow rate are properly chosen. Moreover, the maximum power absorption region becomes smaller as forcing frequency increases and the acoustic wavelength becomes smaller. The results reveal that, in order to maximize the acoustic power being absorbed, both the downstream pipe length and the bias flow rate must be optimized. In summary, the findings from the preliminary tests support the idea that the liner effectiveness (however it may be defined) can be robustly optimized over a broad frequency range by tuning both the downstream length and the bias flow rate.

III. Numerical Investigations of Perforated Liner Damping

A. Description of One-Dimensional Numerical Model

To numerically simulate the preceding experiments, the numerical model developed by Eldredge and Dowling [2] was used. This is a frequency domain code that models the flow fluctuations as being due to plane acoustic waves traveling in opposite directions. The fluctuations are assumed to be linear with respect to the mean flow. The loudspeaker forcing in the experiments is simulated by imposing an inward traveling acoustic wave in one section of the duct (with the amplitude chosen to match that in the experiments). A pressure reflection coefficient at the other end of the duct is used to simulate the open tube end. The acoustic wave strengths within and on either

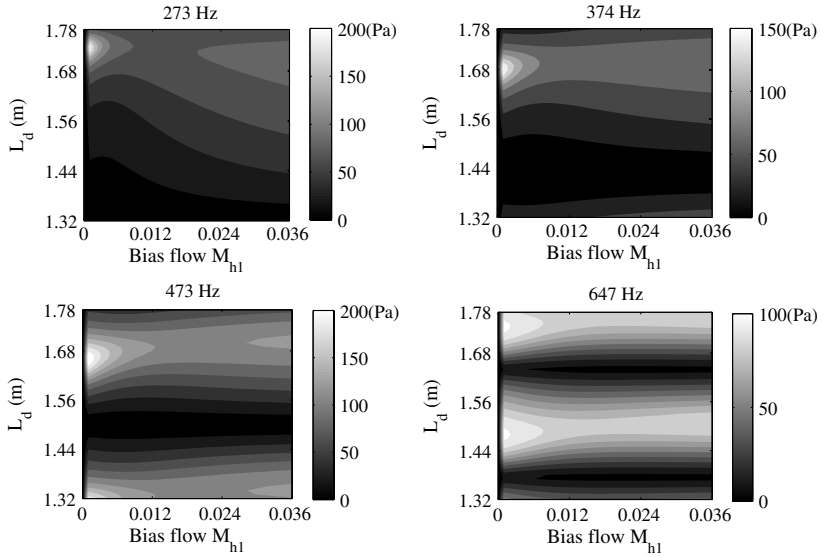

Fig. 6 Pressure amplitude variation at k_4 with downstream pipe length L_d and bias flow Mach number M_{h1}, as M_u is fixed at 0.0.

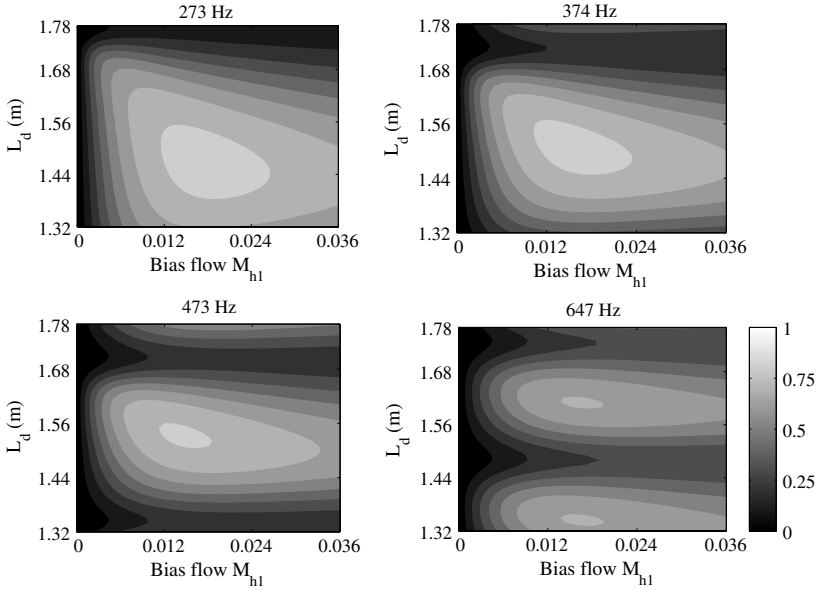

Fig. 7 Power absorption variation with downstream pipe length L_d and bias flow Mach number M_{h1}, as M_u is fixed at 0.0.

Table 2 Comparison between numerical and experimental optimum downstream pipe length L_d and bias flow Mach number M_{h1} for minimizing pressure amplitude at k_4

Frequency, Hz	Experiment L_d, m	Model L_d, m	Experiment M_{h1}	Model M_{h1}
647	1.70	1.69	0.0–0.036	0.0–0.036
473	1.56	1.55	0.0–0.036	0.0–0.036
374	1.44	1.47	0.0–0.036	0.0–0.036

Table 3 Comparison between numerical and experimental optimum downstream pipe length L_d and bias flow Mach number M_{h1} for maximizing power absorption

Frequency, Hz	Experiment L_d, m	Model L_d, m	Experiment M_{h1}	Model M_{h1}
647	1.61	1.60	0.0161	0.0163
473	1.49	1.54	0.0155	0.0157
374	1.50	1.52	0.0149	0.0155

side of the lined section are related using the flow conservation equations along with a homogeneous compliance liner model (adapted from the Rayleigh conductivity for a single aperture).

B. Numerical Simulations

The variations of both the pressure amplitude at k_4 and the power absorption with the bias flow rate and the pipe length are determined numerically and shown in Figs. 6 and 7, respectively. It can be seen from Fig. 6 that the achievable pressure minima is close to 0 Pa at all four frequencies, and the regions of the minimum and maximum pressure amplitudes are periodic in the pipe length L_d. However, the minimum pressure amplitude regions become thinner, as the forcing frequency is increased and the corresponding wave length is decreased. Furthermore, the pressure amplitude depends on the variation of the pipe length much more strongly than the bias flow rate. This is consistent with the measured experimental results. It is noted that the maximum pressure amplitude regions are slightly different from the measured experimental results, as shown in Fig. 4; this is most likely due to the reflection coefficient used in the model. However, qualitatively, the numerical and experimental results are in good agreement.

Figure 7 shows that, as the forcing frequency is increased, the maximum power absorption is slightly deceased. However, to achieve the maximum power absorption, both the pipe length and the bias flow rate need to be properly chosen. All these numerical findings are consistent with experimental ones. It is worth noting that when there is no bias flow (i.e., $M_{h1} = 0.0$), the numerical model shows no acoustic waves being absorbed (i.e., $\Delta = 0$). This is due to the assumption that the liner damping is generated by the vortex shedding excited by the bias flow at the rims of perforated holes. With no mean flow, the liner model has no mechanism for dissipation and reverts to a Rayleigh-type aperture with only an inertial response.

C. Comparison Between Numerical and Experimental Results

To gain insight into the conditions under which the optimum damping occurs, the numerical and experimental results are analyzed and compared. The optimum downstream lengths and bias flow rates for the four different frequencies are summarized in Table 2 for minimizing pressure amplitude at k_4 and in Table 3 for maximizing the power absorption. Table 2 demonstrates that varying bias flow rate has little effect on the pressure amplitude minima at k_4 once the pipe length is properly chosen. Further analysis based on the forcing frequency and speed of sound shows that pressure amplitude minima occur when k_4 is placed near a pressure node.

Table 3 shows that the maximum power absorption depends on both the pipe length and the bias flow rate, with experimental and numerical results agreeing very well. Furthermore, the bias flow Mach number corresponding to maximum power absorption is approximately 0.016 at the three different frequencies, which is close to the theoretical optimum Mach number of 0.021 given by Eq. (5.12) of Eldredge and Dowling [2]. More detailed investigations into how to optimize the liner damping are performed in the following section.

IV. Actively Tuning Perforated Liner Damping

A. Multiple-Parameter Tuning Scheme

To broaden the liners' effective frequency range, both the downstream length and the bias flow rate need to be actively tuned. For this, a multiple-parameter tuning strategy was developed, shown schematically in Fig. 8. It consists of an online identification algorithm, which uses the sensor signal $P(t)$ to predict the main frequency present in the system and its amplitude components at that frequency [13]. That is, it uses an iterative time-domain algorithm, summarized in Eqs. (2a–2c), where n denotes iteration number, to find ω, s, and c, such that $P(t)$ is well approximated by $s \sin \omega t + c \cos \omega t$. This information is fed to a tuning algorithm to determine the optimum actuation signals to alter the downstream pipe length and bias flow rate:

$$\omega_{n+1}^2 = \omega_n^2 + \frac{\omega_n^2 \left[P(t) - P(t - 2\pi/\omega_n)\right]}{\pi \left[s_n \cos \omega_n t - c_n \sin \omega_n\right]} \tag{2a}$$

$$c_n = \frac{\omega_n}{\pi} \int_{t-2\pi/\omega_n}^{t} P(\theta) \cos \omega_n \theta \, \mathrm{d}\theta \tag{2b}$$

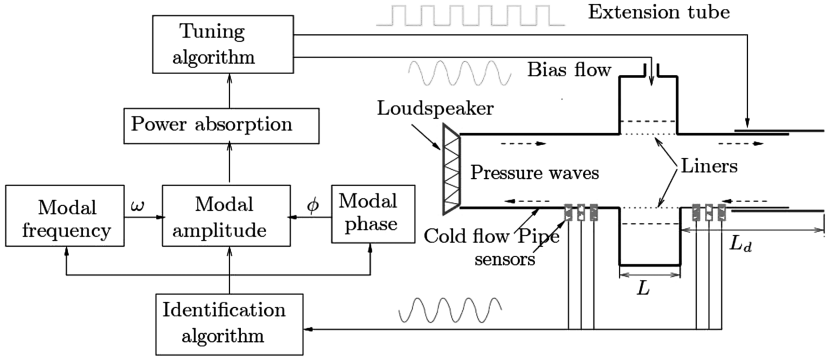

Fig. 8 Multiple-parameter tuning scheme.

$$s_n = \frac{\omega_n}{\pi}\int_{t-2\pi/\omega_n}^{t} P(\theta)\sin\omega_n\theta\,\mathrm{d}\theta \tag{2c}$$

The tuning process initially tunes the downstream length. This can be thought of as placing the liner at an optimum position within the mode shape. Once the downstream length has been tuned, the bias flow rate is then optimized. This process is repeated. The sequential tuning of the two parameters optimizes the liner damping as the frequency present in the system varies. The tuning strategy could be extended to tune a set of perforated liners for damping different modes.

As discussed in Sec. II.B, the acoustic damping of perforated liners can be characterized by either power absorption Δ or pressure amplitude at a given location. To estimate the pressure amplitude at a given location in real time, the mode identification algorithm, as described by Zhao and Morgans [13], is used. To determine the power absorption in real time, the plane waves present in the pipe system need to be decomposed into incident and reflected waves on either side of the lined section. Seybert and Ross [15] developed a two-microphone technique for doing this, involving auto- and cross-spectral density analysis and Fourier transforms. The problem with this approach is that it can only be used at the postprocessing stage rather than in real time. In this work, a real-time version of the two-microphone technique is developed for online decomposition of the plane waves. This is performed in the time domain.

1. *Real-Time Version of Two-Microphone Technique*

Following the approach of Seybert and Ross [15], two pressure measurements at x_1 and x_2 are acquired, as shown in Fig. 9. The measured pressures $p_1(t)$ and $p_2(t)$ are assumed to consist of only one mode at frequency ω, as shown as in Eqs. (3a) and (3b):

$$\begin{aligned} p_1(t) &= \Re\{\hat{p}_1 e^{j\omega t}\} = \Re\{\hat{I}\cdot e^{j(\omega t - k_i x_1)} + \hat{R}\cdot e^{j(\omega t + k_r x_1)}\} \\ &= \Re\{(B_1 - jA_1)e^{j\omega t}\} = A_1\sin(\omega t) + B_1\cos(\omega t) \end{aligned} \tag{3a}$$

$$\begin{aligned} p_2(t) &= \Re\{\hat{p}_2 e^{j\omega t}\} = \Re\{\hat{I}\cdot e^{j(\omega t - k_i x_2)} + \hat{R}\cdot e^{j(\omega t + k_r x_2)}\} \\ &= \Re\{(B_2 - jA_2)e^{j\omega t}\} = A_2\sin(\omega t) + B_2\cos(\omega t) \end{aligned} \tag{3b}$$

where $k_i = \omega/(\bar{c}+\bar{u})$ and $k_r = \omega/(\bar{c}-\bar{u})$ are the incident and reflected wave numbers, $\hat{I}$ and $\hat{R}$ denote the Fourier transforms of the incident and reflected waves amplitudes $I(t)$ and $R(t)$, respectively, $j = \sqrt{-1}$, $\bar{c}$ denotes the speed of sound, $\bar{u}$ is the mean flow velocity, and A_1, B_1, A_2, and B_2 are the amplitude components of $p_1(t)$ and $p_2(t)$. Note that, in the experiment, there is no mean pipe flow (i.e., $\bar{u} = 0$). However, to make the equations more widely applicable to the cases with mean flow, $\bar{u}$ is kept in the equations.

The corresponding Fourier transform of acoustic pressures $\hat{p}_1(\omega)$ and $\hat{p}_2(\omega)$ can be expressed as

$$\hat{p}_1(\omega) = \frac{1}{T}\int_{t-T}^{t} p_1(t)e^{-j\omega t}\,\mathrm{d}t = \hat{I}e^{-jk_i x_1} + \hat{R}e^{jk_r x_1} = \frac{1}{2}(B_1 - jA_1) \tag{4}$$

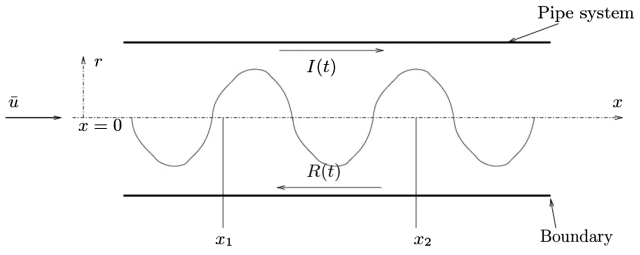

Fig. 9 Schematic of cylindrical pipe with pressure sensors attached.

$$\hat{p}_2(\omega) = \frac{1}{T}\int_{t-T}^{t} p_2(t)e^{-j\omega t}\,\mathrm{d}t = \hat{I}e^{-jk_i x_2} + \hat{R}e^{jk_r x_2} = \frac{1}{2}(B_2 - jA_2) \tag{5}$$

Manipulating Eqs. (4) and (5) gives

$$\begin{pmatrix}\hat{p}_1(\omega)\\ \hat{p}_2(\omega)\end{pmatrix} = \mathbf{Z}\cdot\begin{pmatrix}\hat{I}(\omega)\\ \hat{R}(\omega)\end{pmatrix} \tag{6}$$

$\mathbf{Z}$ is a 2×2 matrix,

$$\mathbf{Z} = \begin{pmatrix} e^{-jk_i x_1} & e^{jk_r x_1} \\ e^{-jk_i x_2} & e^{jk_r x_2}\end{pmatrix} \tag{7}$$

The amplitudes of the decomposed incident and reflected waves can be determined using Eq. (8), where the matrix $\mathbf{Z}$ is assumed to be regular (i.e., nonsingular). Singularity analysis of $\mathbf{Z}$ can be shown to correspond to the two pressure measurements being the same, meaning that it is not possible to uniquely determine the two wave strengths [17,18]:

$$\begin{pmatrix}\hat{I}(\omega)\\ \hat{R}(\omega)\end{pmatrix} = \mathbf{Z}^{-1}\cdot\begin{pmatrix}\hat{p}_1(\omega)\\ \hat{p}_2(\omega)\end{pmatrix} = \mathbf{Z}^{-1}\cdot\begin{pmatrix}\frac{1}{2}[B_1(\omega) - jA_1(\omega)]\\ \frac{1}{2}[B_1(\omega) - jA_1(\omega)]\end{pmatrix} \tag{8}$$

Although the frequency ω and the amplitude components $A_1(\omega)$, $B_1(\omega)$, $A_2(\omega)$, and $B_2(\omega)$ are not known exactly, estimates for them can be provided by the mode identification algorithm, as described by Zhao and Morgans [13]. If the estimates are Ω, $c_1(\Omega)$, $s_1(\Omega)$, $c_2(\Omega)$, and $s_2(\Omega)$, respectively, then the incident and reflected wave amplitudes are obtained in practice using

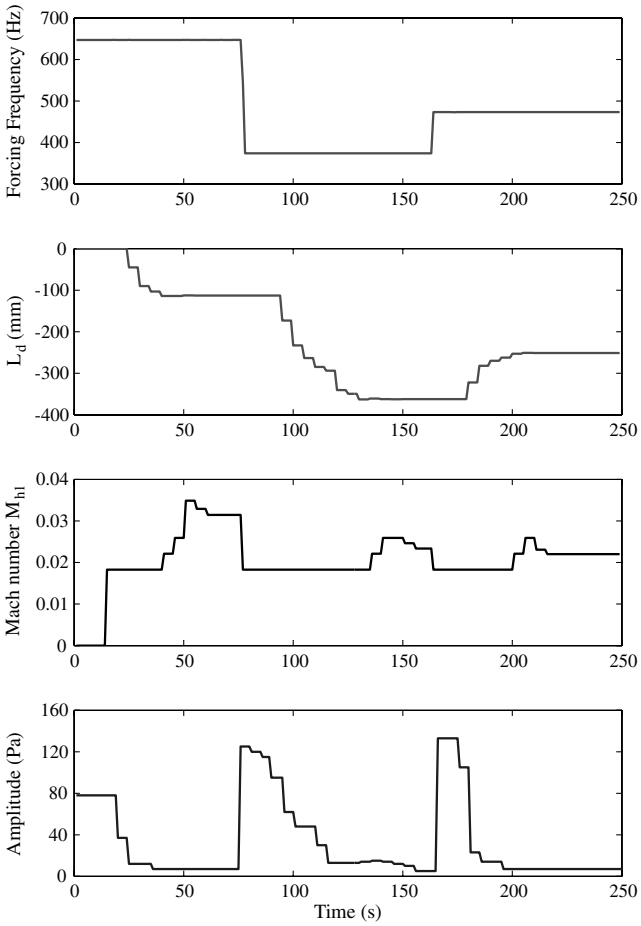

Fig. 10 Minimizing pressure amplitude at *k*4 by tuning both the downstream pipe length and bias flow Mach number as the forcing frequency changes.

$$\begin{pmatrix} \hat{I}(\Omega) \\ \hat{R}(\Omega) \end{pmatrix} = \begin{pmatrix} e^{-j[\bar{\Omega}/(\bar{c}+\bar{u})]x_1} & e^{j[\bar{\Omega}/(\bar{c}-\bar{u})]x_1} \\ e^{-j[\bar{\Omega}/(\bar{c}+\bar{u})]x_2} & e^{j[\Omega/(\bar{c}-\bar{u})]x_2} \end{pmatrix} \cdot \begin{pmatrix} \frac{1}{2}[c_1(\Omega) - js_1(\Omega)] \\ \frac{1}{2}[c_2(\Omega) - js_2(\Omega)] \end{pmatrix} \tag{9}$$

2. Passive Control Algorithm

A passive control algorithm is now developed for determining the optimum actuation signals for the downstream pipe length and the bias flow rate. The core of the control algorithm is a revised Newton–Raphson method used to perform the maximization of the power absorption coefficient or minimization of pressure amplitude, as shown in Eq. (10):

$$v_{n+1} = v_n - \alpha \frac{\partial \hat{q}_{(v)}/\partial v}{\pm|\partial^2 \hat{q}_{(v)}/\partial v^2|} \tag{10}$$

Here, v is the parameter to be optimized, either the downstream pipe length or the bias flow rate. The variable $\hat{q}$ denotes the optimization measure, either the power absorption coefficient or pressure amplitude, and α is a relaxation coefficient to avoid divergence. The full forms of $\partial\hat{q}/\partial v$ and $\partial^2\hat{q}/\partial v^2$ can be found in the work of Wang [19]. Note that, in order to obtain a power absorption maximum, the condition $\partial^2\hat{q}_{(v)}/\partial v^2 < 0$ implies that the + sign in Eq. (10) must be taken, while to obtain a pressure amplitude minimum, the condition $\partial^2\hat{q}_{(v)}/\partial v^2 > 0$ implies choosing the − sign.

B. Performance of Multiple-Parameter Tuning Approach

The multiple-parameter tuning scheme is implemented in LabVIEW 8.50, with the data acquisition system consisting of a National Instruments PCI-6229 card and two BNC 2090 connectors. Its effectiveness in optimizing the damping performance of the liner is evaluated.

1. Minimizing Pressure Amplitude

The cold-flow pipe system was acoustically forced using the loudspeaker mounted at one end. The forcing frequency was varied significantly in time, as shown in the top graph of Fig. 10, to simulate the effect of changing operating conditions. Even though, in the experiment, the forcing frequency is known exactly, this would not be true for a general combustion system, and so the frequency was assumed unknown in the tuning algorithms. The aim of the tuning was to obtain and maintain minimum pressure amplitude at k_4 as these frequency changes occurred.

The measured pressure perturbation at k_4 is analyzed using the online algorithm described in the work of Zhao and Morgans [13]. This provides a continually updated estimate of the frequency and pressure amplitude present at k_4. This information is fed into the control algorithm so that the downstream pipe length L_d and bias flow rate M_{h1} can be tuned so as to minimize the pressure amplitude at k_4.

Figure 10 presents the sequence of the variation of the forcing frequency, the tuning process (middle graphs), and the effect of tuning in terms of pressure amplitude (bottom graph). Initially, the forcing frequency is 647 Hz. When the tuning algorithm is switched

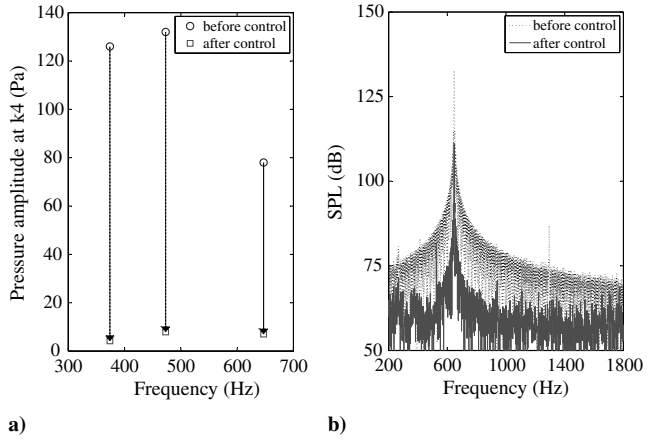

Fig. 11 Pressure amplitude reduction at $k4$ and the corresponding sound pressure level (SPL) reduction at 647 Hz.

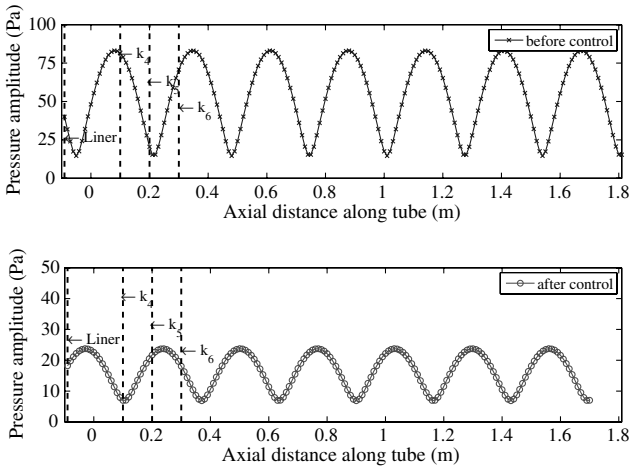

Fig. 12 Mode shape before and after minimizing the pressure amplitude at k_4 at a forcing frequency of 647 Hz.

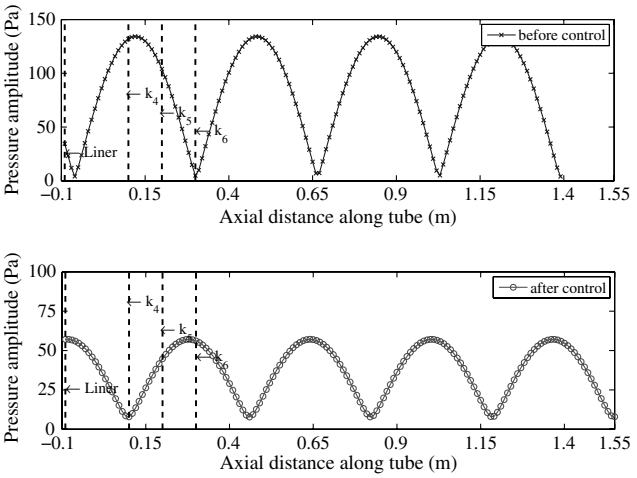

Fig. 13 Mode shape before and after minimizing the pressure amplitude at k_4 at a forcing frequency of 473 Hz.

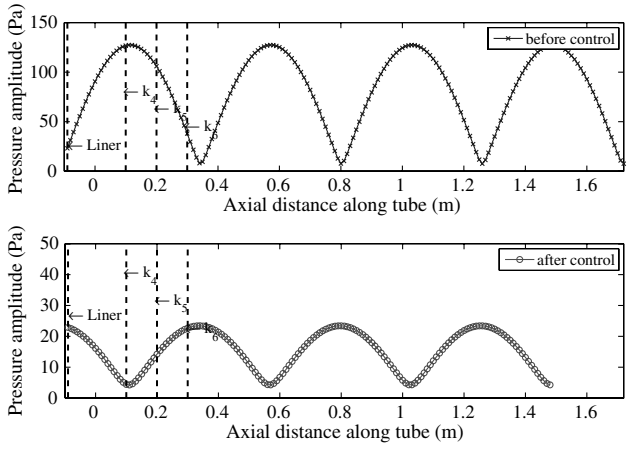

Fig. 14 Mode shape before and after minimizing the pressure amplitude at k_4 at a forcing frequency of 374 Hz.

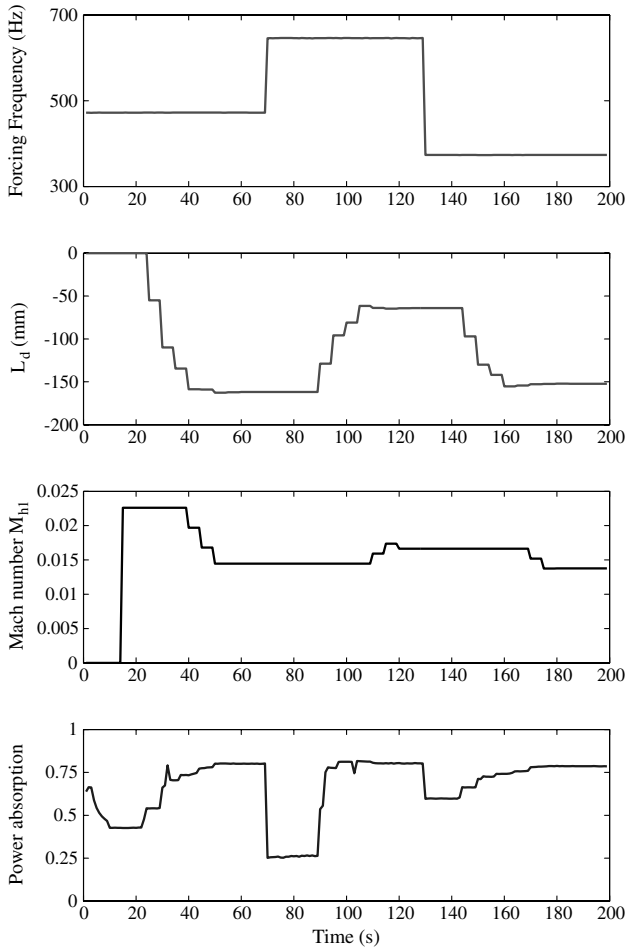

Fig. 15 The variation of forcing frequency, downstream pipe length, bias flow Mach number and power absorption with time.

on at $t = 25$ s, the downstream length and bias flow rate both successively adapt from starting values of 1790 mm and 6 m/s, so that within 25 s, the pressure amplitude at k_4 has been minimized to approximately 5 Pa. Note that the speed of tuning in the experiment was limited by the stepper motor and centrifugal pump. At $t = 70$ s, the forcing frequency is changed to 374 Hz. The downstream length and bias flow rate retune to reduce the pressure amplitude corresponding at the new forcing frequency. At $t = 130$ s, the forcing frequency is changed again, this time to 473 Hz. Once again, the pressure amplitude is minimized via tuning the downstream length and bias flow rate. Thus, it can be seen that the downstream length and bias flow rate are successfully tuned to maintain a small pressure amplitude at k_4, even for very large changes in the main frequency present. It is noted that, while the optimum downstream length depends very much on the forcing frequency, the optimum bias flow rate varies little. This is consistent with the findings from the preliminary experimental tests and numerical simulations.

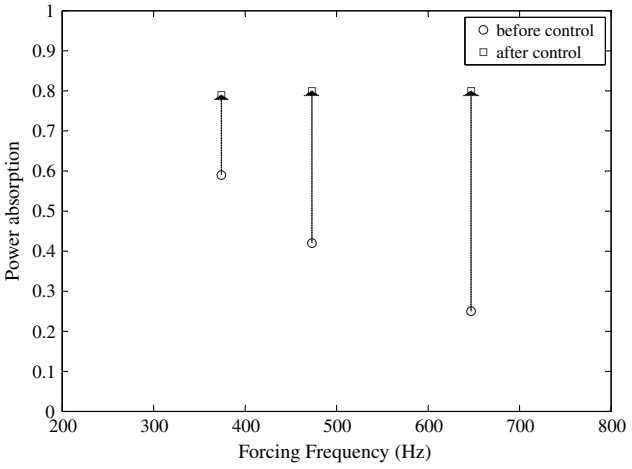

Fig. 16 Improvement in power absorption obtained by the tuning algorithm at each of the three forcing frequencies.

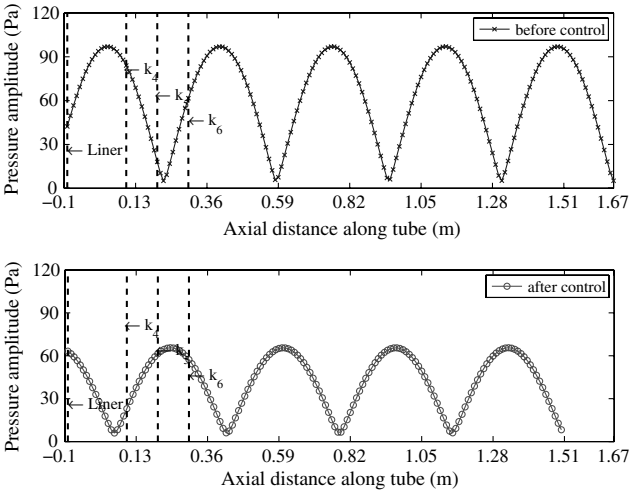

Fig. 17 Mode shape before and after maximizing the power absorption at a forcing frequency of 473 Hz.

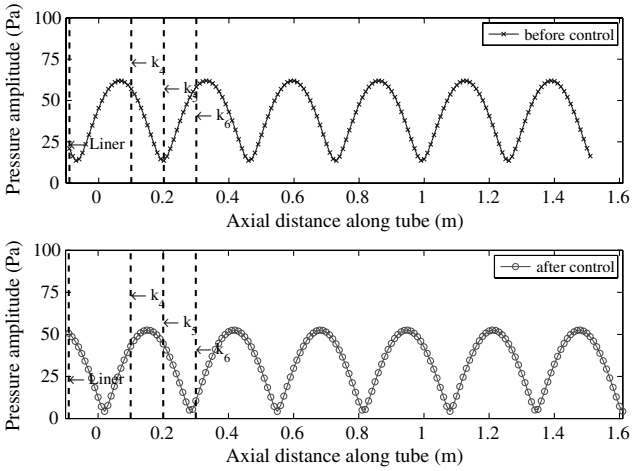

Fig. 18 Mode shape before and after maximizing the power absorption at a forcing frequency of 647 Hz.

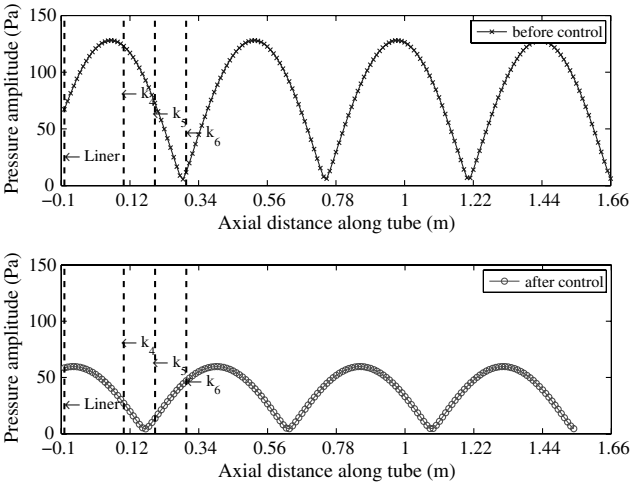

Fig. 19 Mode shape before and after maximizing the power absorption at a forcing frequency of 374 Hz.

Figure 11a presents the reduction in the pressure amplitude at k_4 obtained at each of the three frequencies by the multiple-parameter tuning. A significant reduction is obtained at all three frequencies. The effect of this reduction on the pressure spectrum at k_4 is shown in Fig. 11b (for excitation at 647 Hz).

To gain insight into the conditions under which the minimum pressure amplitude occurs, the mode shape along the pipe was obtained before and after control using the two-microphone technique at each of the three forcing frequencies. The mode shapes before and after tuning are shown in Figs. 12–14 at each of the three forcing frequencies. It can be seen that, at each frequency, the effect of the tuning is to place k_4 at a pressure node, as expected. Moreover, the amplitude of acoustic waves downstream of the lined section is significantly reduced after tuning. Note that the pressure amplitude at the open end after tuning is approximately 5 Pa rather than exactly 0 Pa. This is most likely due to the end correction effect [8].

2. *Maximizing Power Absorption*

The multiple-parameter tuning strategy is now used to experimentally maximize the power absorption provided by the perforated liner. Figure 15 presents the sequence of frequency changes, the resulting tuning of the parameters L_d and M_{h1}, and the effect of this tuning on the power absorption. Initially, the forcing frequency is 473 Hz. When the tuning algorithm is switched on at $t = 25$ s, the downstream length and bias flow rate both successively adapt from starting values of 1670 mm and 7 m/s, so that within 25 s, the power absorption has been maximized to approximately 80%. At $t = 70$ s, the forcing frequency is changed to 647 Hz. The downstream length and bias flow rate retune to give maximum power absorption at the new frequency. At $t = 130$ s, the forcing frequency is changed again to 374 Hz, and the tuning results in the power absorption again being maximized. The change in the power absorption provided by the tuning at each frequency is summarized in Fig. 16. It is clear that the tuning is successful in maintaining peak power absorption, even for large changes in the system frequency.

The mode shapes before and after tuning are shown in Figs. 17–19. It can be seen in each case that maximum power absorption occurs when the liner (i.e., the axial centerline of the lined section) is located at a pressure antinode. These findings are found to be consistent with the numerical findings from Eldredge and Dowling [2].

V. Conclusions

For different applications, the damping effect of perforated liners can be characterized using either pressure amplitude at a prescribed location (such as at the flame position) or the degree to which acoustic waves are absorbed (i.e., power absorption). It has been shown, experimentally and using a numerical model, that the damping of a liner can be altered by varying two parameters: a pipe length scale and the bias flow rate through the perforated holes. When expressing the liner damping in terms of pressure amplitude at a given location, the dependence on pipe length is much stronger than the dependence on bias flow rate. When power absorption is used, the liner performance is strongly dependent on both the bias flow rate and the pipe length. Design guidance insights, in terms of the mode shapes that give the optimum pipe lengths and bias flow rates, have been obtained.

To maintain the damping performance of a perforated liner in the presence of a varying instability frequency, a multiple-parameter tuning was performed, using a strategy that first tuned the downstream pipe length and then the bias flow rate successively. The tuning strategy consists of a revised Newton–Raphson algorithm that seeks to optimize the liner damping effect. The liner damping was tracked in real time using a combination of the mode identification algorithm, developed by Zhao and Morgans [13], and a real-time version of the two-microphone technique, developed especially for this experiment.

On implementing the tuning algorithms, it was found that the downstream pipe length and the bias flow rate could be successively optimized to give either maximum power absorption or minimum pressure amplitude. It was seen that maximum power absorption corresponded to placing the liner at a pressure antinode, while minimum pressure amplitude corresponded to the measurement location being placed at a pressure node.

The reported investigation was undertaken in a cold-flow pipe system in which both the bias flow rate and the pipe length could be varied so as to optimize the liner damping. Although, in a real combustion system, it would be difficult to alter the combustor length, a similar effect can be achieved by varying the combustor boundary condition [20], as this also results in the changes of the mode shape.

Appendix: Assessing Perforated Liner Damping Effect Using Transmission Coefficient

In some applications, perforated liners are implemented as acoustic dampers to prevent reflected acoustic waves in the pipe/combustor from transmitting back to the noise source (e.g., flame), thus alleviating the growth of acoustically driven instabilities. For this, the fraction of the acoustic wave energy that is transmitted

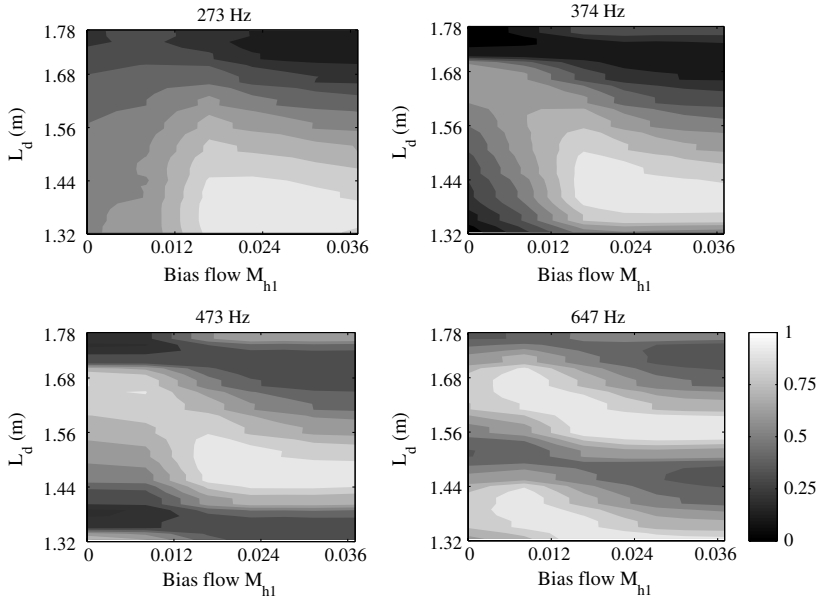

Fig. A1 Variations of transmission coefficient, β with the pipe length, L_d and bias flow rate, M_{h1}, as measured experimentally, with M_u fixed at 0.0.

downstream of the lined section (i.e., the transmission coefficient β) can be used as an alternative to access the liner damping effect. The variation of the transmission coefficient β, defined as $\beta = 1.0 - |\hat{R}_u(\omega)|^2/|\hat{I}_u(\omega)|^2$, with the bias flow rate and the pipe length is shown in Figure A1 at four different frequencies. It can be seen that the transmission coefficient depends on both the pipe length and the bias flow rate. The maximum transmission coefficient can thus also be achieved by choosing both the pipe length and the bias flow rate appropriately.

Acknowledgments

Dan Zhao's Ph.D. research was financially supported by the C. T. Taylor Fund, the Lundgren Research Fund, the Cambridge Overseas Trust, the Cambridge University Board of Graduate Studies, and Darwin College. Aimee Morgans was supported as a Research Fellow by the Royal Academy of Engineering and the Engineering and Physical Sciences Research Council. This financial support is gratefully acknowledged. The authors thank John Hazelwood for his technical support in this work.

References

[1] Lieuwen, T. C., and Yang, V., *Combustion Instabilities in Gas Turbine Engines*, AIAA, Reston, VA, 2005, pp. 3–24.

[2] Eldredge, J. D., and Dowling, A. P., "The Absorption of Axial Acoustic Waves by a Perforated Liner with Bias Flow," *Journal of Fluid Mechanics*, Vol. 485, 2003, pp. 307–335. doi:10.1017/S0022112003004518

[3] Heuwinkel, C., Enghardt, L., and Rohle, I., "Concept and Experimental Investigation of a Zero Mass Flow Liner," AIAA Paper 2008-2931, 2008.

[4] Jing, X. D., and Sun, X. F., "Experimental Investigations of Perforated Liners with Bias Flow," *Journal of the Acoustical Society of America*, Vol. 106, No. 5, 1999, pp. 2436–2441. doi:10.1121/1.428128

[5] Jing, X. D., and Sun, X. F., "Effect of Plate Thickness on Impedance of Perforated Plates with Bias Flow," *AIAA Journal*, Vol. 38, No. 9, 2000, pp. 1573–1578. doi:10.2514/2.1139

[6] Follet, J. I., Betts, J. F., and Kelly, J. J., "Improvements to Acoustic Liner Broadband Absorption Using Bias Flow," AIAA Paper 2001-0823, 2001.

[7] Reichert, R. S., and Biringen, S., "Time-Domain Simulation of Acoustic Propagation in a Lined Duct," *Applied Acoustics*, Vol. 62, No. 9, 2001, pp. 1049–1068. doi:10.1016/S0003-682X(00)00090-6

[8] Morse, P. M., and Ingard, K. U., *Theoretical Acoustics*, Princeton Univ. Press, Princeton, NJ, 1987, pp. 467–492.

[9] Tam, C. K. W., Kurbatskii, K. A., Ahuja, K. K., and Gaeta, R. J., "A Numerical and Experimental Investigation of the Dissipation Mechanisms of Resonant Acoustic Liners," *Journal of Sound and Vibration*, Vol. 245, No. 3, 2001, pp. 545–557. doi:10.1006/jsvi.2001.3571

[10] Howe, M. S., "On the Theory of Unsteady High Reynolds Number Flow Through a Circular Aperture," *Proceedings of the Royal Society of London A*, Vol. 366, 1979, pp. 205–223. doi:10.1098/rspa.1979.0048

[11] Hughes, I. J., and Dowling, A. P., "The Absorption of Sound by Perforated Linings," *Journal of Fluid Mechanics*, Vol. 218, 1990, pp. 299–335. doi:10.1017/S002211209000101X

[12] Zhao, D., Barrow, C., Morgans, A. S., and Carrotte, J., "Acoustic Damping of a Helmholtz Resonator with an Oscillating Volume," *AIAA Journal*, Vol. 47, No. 7, 2009, pp. 1672–1679. doi:10.2514/1.39704

[13] Zhao, D., and Morgans, A. S., "Tuned Passive Control of Combustion Instabilities Using Multiple Helmholtz Resonators," *Journal of Sound and Vibration*, Vol. 320, Nos. 4–5, 2009, pp. 744–757. doi:10.1016/j.jsv.2008.09.006

[14] Chung, J. Y., and Blaser, D. A., "Transfer Function Method of Measuring In-Duct Acoustic Properties, II: Experiment," *Journal of the Acoustical Society of America*, Vol. 68, No. 3, 1980, pp. 914–921. doi:10.1121/1.384779

[15] Seybert, A. F., and Ross, D. F., "Experimental Determination of Acoustic Properties Using a Two-Microphone Random-Excitation Technique," *Journal of the Acoustical Society of America*, Vol. 61, No. 5, 1977, pp. 1362–1370. doi:10.1121/1.381403

[16] Chung, J. Y., and Blaser, D. A., "Transfer Function Method of Measuring In-Duct Acoustic Properties, I: Theory," *Journal of the Acoustical Society of America*, Vol. 68, No. 3, 1980, pp. 907–913. doi:10.1121/1.384778

[17] Seybert, A. F., and Soenarko, B., "Error Analysis of Spectral Estimates with Application to the Measurement of Acoustic Parameters Using Random Sound Fields in Ducts," *Journal of the Acoustical Society of America*, Vol. 69, No. 4, 1981, pp. 1190–1199. doi:10.1121/1.385700

[18] Abom, M., and Boden, H., "Error Analysis of Two-Microphone Measurements in Ducts with Flow," *Journal of the Acoustical Society of America*, Vol. 83, 6, 1988, pp. 2429–2438. doi:10.1121/1.396322

[19] Wang, C.-H., "Actively-Tuned Passive Control of Combustion Instabilities," Ph.D. Dissertation, Department of Engineering, Univ. of Cambridge, Cambridge, England, U.K., 2004.

[20] Bothien, M. R., Moeck, J. P., and Paschereit, C. O., "Active Control of the Acoustic Boundary Condition of Combustion Test Rigs," *Journal of Sound and Vibration*, Vol. 318, Nos. 4–5, 2008, pp. 678–701. doi:10.1016/j.jsv.2008.04.046

J. Astley
Associate Editor